Supporting Information (SI)

to

Disposable Saliva Electrochemical MIP-based Biosensor for Detection of Stress Biomarker α-amylase in Point-of-care

Tânia S.C.R. Rebelo, Inês M. Miranda, Ana T.S.C. Brandão, Laura I.G. Sousa, José A. Ribeiro*, A. Fernando Silva, Carlos M. Pereira*

CIQUP – Chemistry Research Center, Department of Chemistry and Biochemistry, Faculty of Sciences of University of Porto

Rua do Campo Alegre 687, s/n, Porto 4169-007, Portugal

*) **Corresponding Authors**

E-mail: jose.ribeiro@fc.up.pt (J.A. Ribeiro), cmpereir@fc.up.pt (C.M. Pereira).

Results and Discussion

Randle's equivalent circuit

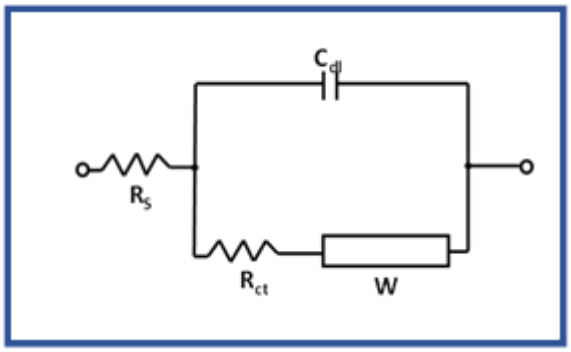

Fig. S1. Schematic representation of Randle's equivalent circuit.

This circuit is composed by the solution resistance (R_s), the double layer capacitance (C_{dl}), the charge transfer resistance (R_{ct})), which is inversely proportional to the rate of electron transfer at the electrode surface, and a Warburg element (W), related to the diffusion of ions from the bulk electrolyte to the electrode interface [1, 2].

A typical Nyquist plot includes a semicircle, at high frequency region due to a charge-transfer controlled behaviour, followed by a straight line, at low frequency region displaying a diffusion-controlled behaviour. Interpretation of the impedance data requires the use of equivalent circuits which will enable to extract of R_{ct} values for all process steps (easily evaluated by the size of the semi-circle) [3].

Table S1. Fitting parameters extracted from electrochemical impedance data using the Randles type equivalent circuit.

Parameters	Bare Au	CA SAM	α-amylase immobilization	Electropolymerization	After template extraction
R_s (Ω)	4.1×10^{1}	2.9×10^{1}	2.8×10^{1}	3.6×10^{1}	3.6×10^{1}
Q (Ω^{-1} s^{-n})	2.5×10^{-5}	2.5×10^{-5}	2.4×10^{-5}	1.7×10^{-5}	1.9×10^{-5}
n	0.94	0.96	0.95	0.96	0.95
R_{ct} (Ω)	5.2×10^{2}	5.2×10^{2}	8.6×10^{2}	1.3×10^{5}	5.1×10^{4}
W (Ω $s^{-1/2}$)	3.4×10^{-3}	2.1×10^{-3}	2.8×10^{-3}	2.7×10^{-3}	2.7×10^{-3}

Optimization of the MIP film thickness

In order to evaluate the impact of the number of CV cycles (one, two and 15) performed during the electropolymerization process (film thickness) on the MIP performance, EIS measurements were performed (at fixed α-amylase concentration of 12 μg mL^{-1}) before and after extraction of template from the polymeric matrix. The results are shown in Fig.S2.

From the results obtained, we can conclude that one CV cycle during Py electropolymerization (Fig. S2A) was enough to produce a responsive sensor (lower value of R_{ct} after formation of the MIP), since it allowed the effective removal of the target molecule from the ultrathin polymeric matrix. When thicker films were built, by performing two and 15 CV cycles, the extraction procedure was not successful, imposing a lack of sensitivity (high R_{ct} values) due to limited number (or absence) of specific cavities at the MIP film surface.

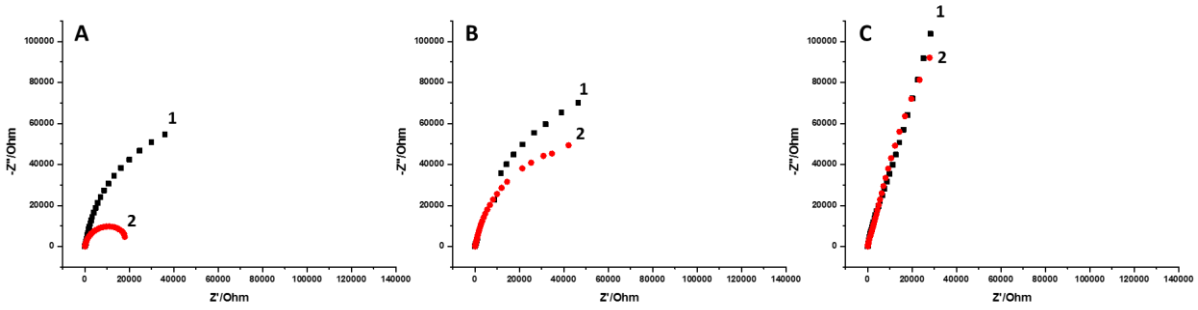

Fig. S2. EIS plots, obtained in the presence of 5.0 mmol L^{-1} $[Fe(CN)_6]^{3-/4-}$ redox couple, (curves 1) after electropolymerization and (curves 2) after template protein extraction from the polymer matrix (by surface incubation with a 25 mmol L^{-1} SDS solution overnight), for the different number of CV cycles performed during the electropolymerization process: (A) 1 cycle, (B) 2 cycles and (C) 15 cycles.

Methodologies reported in literature for α-amylase detection in saliva

Table S2. Analytical features of detection methodologies reported in the literature for detection of α-amylase.

Detection methodology	**Response range (mg mL^{-1})**	**LOD (mg mL^{-1})**	**Reference**
Imaging capillary isoelectric focusing	0.2 - 1	---	[4]
Potentiometric biosensor	1.4 - 45.5$^{(*)}$	$5.5\times10^{-3(*)}$	[5]
Tri-enzymatic amperometric biosensor	0.23 - 11.4$^{(*)}$	0.23$^{(*)}$	[6]
Impedance spectroscopy and QCM	3.6×10^{-3} - 0.36	3.6×10^{-4}	[7]
QCM-based immunosensor	1×10^{-3} - 0.1	1.3×10^{-4}	[8]
Electrochemical MIP-based detection	3.0×10^{-4} - 0.60	$<3.0\times10^{-4}$	This work

(*) Value were obtained by considering 22 U =1 mg [9].

Reusability

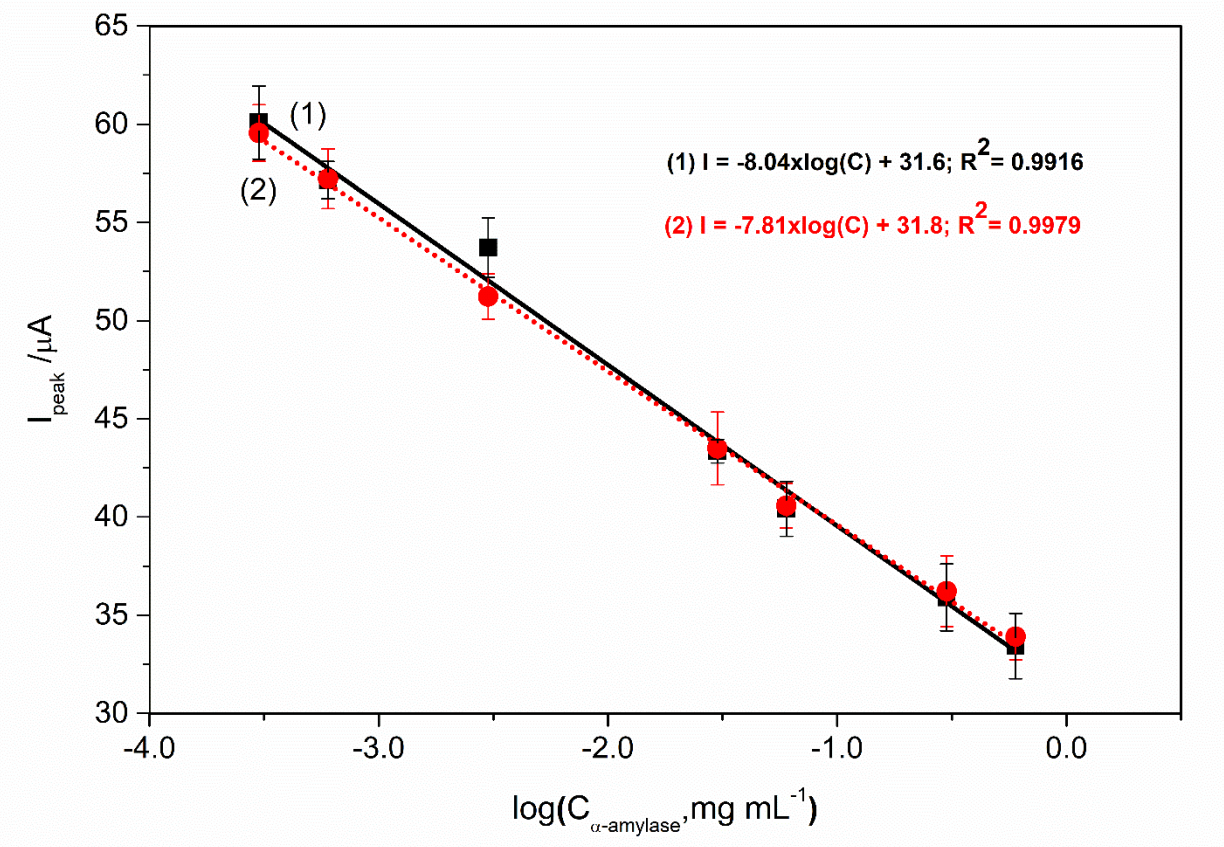

Fig. S3. Calibration curves displaying the effect of reusability of the same MIP-based biosensor for two independent assays.

Selectivity and application of the MIP-based biosensor

A simple method was used to avoid inference from native α-amylase in saliva samples in recovery studies. It consisted to irreversible denature the protein by elevated temperature (>85°C) [10] and posterior confirmation by Lugol test (colorimetric assay) [9, 11]. Lugol iodine, also known as Lugol solution, is often used as a reagent for starch detection in routine laboratory and medical tests. This solution is used as an indicator for the presence of starches in organic compounds. Lugol iodine reacts with starch to give a dark blue-black color. Thus, the protein denaturation process was followed by hydrolysis (or not) of starch by salivary α-amylase to produced simple sugars as function of the temperature (see Fig. S4).

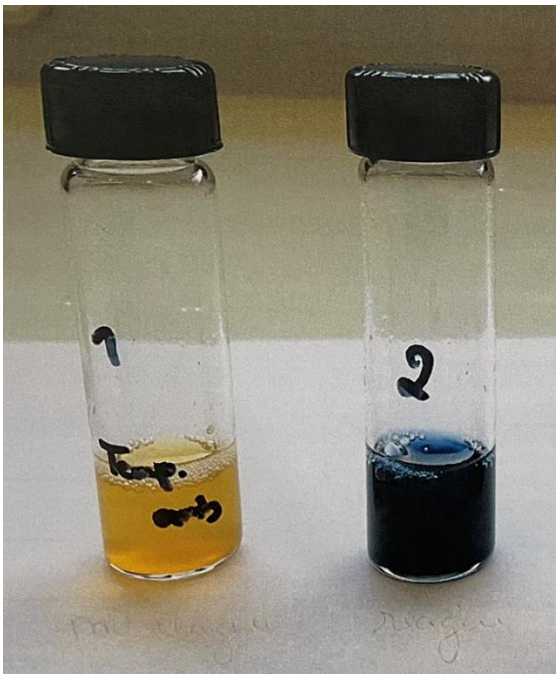

Fig. S4. Typical colors obtained after Lugol test in a mixture of 1 mL saliva + 1 mL starch. Tube 1: saliva sample previous boiled (T = 100 ºC for 10 min) for enzyme denaturation; Tube 2: Control saliva sample (temperature controlled hydrolysis at 37 ºC for 10 min).

Table S3. Determination of α-amylase in human saliva.

Sample	α-amylase added (mg mL^{-1})	α-amylase found (mg mL^{-1})	Recovery (%)	Relative error (%)
1	6.50×10^{-4}	$7.0\times10^{-4} \pm 2\times10^{-5}$	92.3 ± 2.6	-8.3
2	6.50×10^{-3}	$6.07\times10^{-3} \pm 4\times10^{-5}$	107.0 ± 0.8	6.6
3	1.50×10^{-2}	$1.31\times10^{-2} \pm 8\times10^{-5}$	114.2 ± 0.7	12.4

Template protein extraction – preliminary ESI studies

Preliminary EIS experiments were performed at the NIP surface aiming to evaluate its stability under the extraction conditions tested. The impedance results obtained are shown in Fig. S5. As can be seen in the Fig. S5A, similar charge transfer resistance (R_{tc}) values were obtained before and after surface treatment with SDS solution meaning that NIP surface integrity was preserved (Fig. S5A). By opposition, lower R_{ct} values were obtained after NIP surface treatment with H_2SO_4 (Fig. S5B) and NaOH (Fig. S5C) which may indicate a possible damage of the polymer (and removal from the electrode surface) induced by the extraction solutions. So, SDS solution was chosen in this work for effective removal of the template from polymeric matrix.

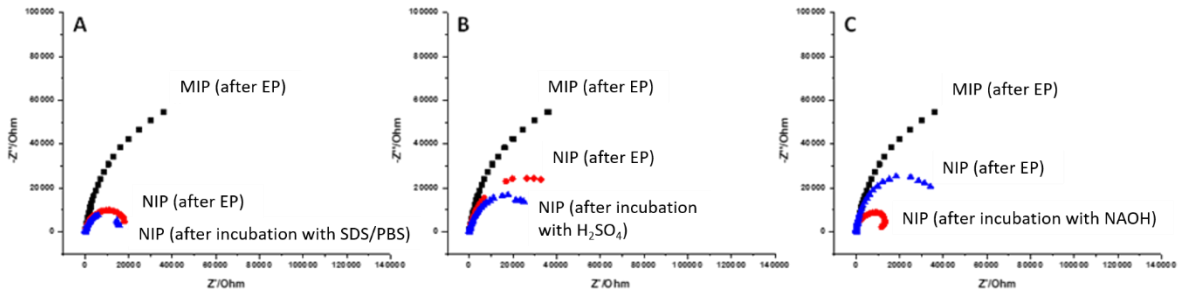

Fig. S5 - EIS spectra, obtained in the presence of 5 mM $[Fe(CN)_6]^{3-/4-}$, at the MIP/NIP surfaces before and after surface treatment with the different extraction solutions tested: A-SDS, B-H_2SO_4 and C-NaOH.

References

1. Moreira, F. T. C.; Dutra, R. A. F.; Noronha, J. P. C.; Sales, M. G. F., Electrochemical biosensor based on biomimetic material for myoglobin detection. *Electrochimica Acta* **2013,** *107* (0), 481-487.

2. Moreira, F. T. C.; Sharma, S.; Dutra, R. A. F.; Noronha, J. P. C.; Cass, A. E. G.; Sales, M. G. F., Protein-responsive polymers for point-of-care detection of cardiac biomarker. *Sensors and Actuators B: Chemical* **2014,** *196* (0), 123-132.

3. Panagopoulou, M. A.; Stergiou, D. V.; Roussis, I. G.; Prodromidis, M. I., Impedimetric Biosensor for the Assessment of the Clotting Activity of Rennet. *Analytical Chemistry* **2010,** *82* (20), 8629-8636.

4. Zarabadi, A. S.; Huang, T.; Mielke, J. G., Capillary isoelectric focusing with whole column imaging detection (iCIEF): A new approach to the characterization and quantification of salivary α-amylase. *Journal of Chromatography B* **2017,** *1053* (Supplement C), 65-71.

5. Zhang, L.; Yang, W.; Yang, Y.; Liu, H.; Gu, Z., Smartphone-based point-of-care testing of salivary α-amylase for personal psychological measurement. *Analyst* **2015,** *140* (21), 7399-7406.

6. Mahosenaho, M.; Caprio, F.; Micheli, L.; Sesay, A. M.; Palleschi, G.; Virtanen, V., A disposable biosensor for the determination of alpha-amylase in human saliva. *Microchimica Acta* **2010,** *170* (3), 243-249.

7. Gibbs, M. J.; Biela, A.; Krause, S., α-Amylase sensor based on the degradation of oligosaccharide hydrogel films monitored with a quartz crystal sensor. *Biosensors and Bioelectronics* **2015,** *67*, 540-545.

8. Della Ventura, B.; Sakač, N.; Funari, R.; Velotta, R., Flexible immunosensor for the detection of salivary α-amylase in body fluids. *Talanta* **2017,** *174* (Supplement C), 52-58.

9. Dutta, S.; Mandal, N.; Bandyopadhyay, D., Paper-based α-amylase detector for point-of-care diagnostics. *Biosensors and Bioelectronics* **2016,** *78*, 447-453.

10. Singh, K.; Shandilya, M.; Kundu, S.; Kayastha, A. M., Heat, Acid and Chemically Induced Unfolding Pathways, Conformational Stability and Structure-Function Relationship in Wheat α-Amylase. *PLOS ONE* **2015,** *10* (6), e0129203.

11. Valls, C.; Rojas, C.; Pujadas, G.; Garcia-Vallve, S.; Mulero, M., Characterization of the activity and stability of amylase from saliva and detergent: Laboratory practicals for studying the activity and stability of amylase from saliva and various commercial detergents. *Biochemistry and Molecular Biology Education* **2012,** *40* (4), 254-265.